Desalination and Water Treatment
www.deswater.com
doi: 10.1080/19443994.2015.1086894

57 (2016) 17570–17578
August

Taylor & Francis
Taylor & Francis Group

Kinetic and computational evaluation of activated carbon produced from rubber tires toward the adsorption of nickel in aqueous solutions

Mohammad N. Siddiqui[a,*], Halim H. Redhwi[b], Abdulaziz A. Al-Saadi[a], Mohammed Rajeh[a], Tawfik A. Saleh[a]

[a]*Chemistry Department, King Fahd University of Petroleum & Minerals, Dhahran 31261, Saudi Arabia, Tel. +966 13 8602529; emails: mnahid@kfupm.edu.sa (M.N. Siddiqui), asaadi@kfupm.edu.sa (A.A. Al-Saadi), mrnsmrvip@gmail.com (M. Rajeh), tawfik@kfupm.edu.sa (T.A. Saleh)*
[b]*Chemical Engineering Department, King Fahd University of Petroleum & Minerals, Dhahran 31261, Saudi Arabia, email: hhamid@kfupm.edu.sa*

Received 1 January 2015; Accepted 14 August 2015

ABSTRACT

This work aims to evaluate the potential of waste rubber tire as an inexpensive sorbent material for nickel ion removal from aqueous solution. A laboratory scale study carried out on the production of activated carbon (AC) from waste rubber tire by physical activation method. Scanning electron microscope analysis was used to characterize the surface properties of the AC adsorbent. The surface area of AC was measured to be 465 m^2/g. This large surface area of the AC could play a vital role in enhancing the removal of Ni(II). Aqueous solutions containing nickel ion in varying concentrations were prepared. Batch adsorption experiments at different operating parameters such as pH, metal concentration, adsorbent dose, contact time and temperature were carried out. These in turn revealed the adsorption capacity and helped in determining the mechanism with respect to thermodynamics, equilibrium and kinetics. The kinetic studies were carried out to determine the kinetics of the adsorption process. The Langmuir isotherm was followed under the present conditions with $R^2 = 0.938$. The overall absolute deviations between experimental and predicted values were found to be 14.4%. The Langmuir model better appears to fit the adsorption of Ni onto AC adsorbent. The characterization and computational studies of the AC adsorbent after adsorption of nickel was also carried out and the results confirmed the positive adsorption process. FTIR analysis of AC before and after Ni adsorption indicated that adsorption of nickel metal on AC took place with the disappearance/diminishing of carbonyl groups. The results of nickel adsorption on AC revealed its potential for pollutant removal and finally its application in water treatment.

Keywords: Nickel; Activated carbon; Adsorption; Kinetic studies; Computational studies

1. Introduction

Porous structures resulting in high surface area is considered as the most important property of a good adsorbent. In addition, the time taken for adsorption equilibrium to be established should be as small as possible so that it can be used to remove contaminants in lesser time. Thus, adsorbents with high surface area and porosity and showing fast adsorption kinetics are

*Corresponding author.

used for the removal of pollutants. The phenomenon of adsorption was observed in 1,773 for gases exposed to carbon, that was followed by observations made by Lowitz in 1,785 of the reversible removal of colour- and odour-producing compounds from water by wood charcoal [1]. Similar phenomenon was observed with vegetable and animal charcoals, respectively. The versatility and wide applicability of adsorption in pollution control has been recognized [2]. The importance of adsorption [3,4] in the chemical, food, petroleum, and pharmaceutical industries is also well established. A variety of solid adsorbents have been developed and used for removing solutes from solution by adsorption [5].

Activated carbon (AC) remains the most widely studied adsorbent, and it has been found to adsorb a variety of materials such as metals, dyes, phenols, and a host of other organic compounds and bio-organisms, and is, therefore, used for the removal of pollutants from wastewaters by adsorption. The design and operation of the process is convenient and can be handled easily, and the operational costs are therefore comparatively low. As a result, the cost of the adsorbent, and the additional costs of regeneration if required, can be a significant fraction of the overall process costs [6]. The materials that have been investigated for this purpose include both natural, wastes materials and by-products generated from many industries [7].

In an attempt to overcome the economic disadvantages of AC, wood as an adsorbent was investigated for the removal of telon blue [8]. Natural coal was studied [9] as an adsorbent for the removal of dyes. In a study of removal and recovery of Cu(II), Cr(III) and Ni(II) from solutions, Chui et al. [10] utilized crude shrimp chitin as a low-cost adsorbent. McKay et al. [11] reported the adsorption capacity of Fuller's earth for basic and acid blue. In addition to the above-discussed natural materials, the number of workers has also investigated a number of agricultural wastes/industrial by-products as adsorbents for the removal of pollutants. Some of the adsorbents as reported in literature are peanut hull [12], hazelnut shells, almond shell, olive stones, and peach stones [13] rubber seed coat [14], blast furnace sludge [15–19] studied different adsorbents for different pollutants and sewage sludge [20].

After the critical evaluation of the reported work, it was observed that most adsorbents show poor adsorption capacities, longer equilibration times, and maximum adsorptions at extreme pH values. Moreover, the management of the exhaustive adsorbent is a very serious concern, which has not been considered in the previous reported papers. Besides, the developed adsorbents have not been tested for different pollutants, especially under column studies. In addition to this, many waste by-products have not been used for the preparation of adsorbents. Briefly, a lot of work is required in this direction of the low-cost alternatives to carbon. The AC is used for the tertiary treatment of wastewater in many industries, for example, food, textile, chemical and pharmaceutical industries [21]. In some applications, large molecules or macromolecules cannot penetrate into the micropores (<2 nm diameter) and adsorb onto them, so the produced ACs should possess not only micropores, but also interconnecting mesopores [22]. In particular, it was shown that, amongst the solid wastes, ACs prepared from PET and waste tires are highly mesoporous and have remarkably high adsorption capacity for large molecules [23]. Due to this reason, waste tires give another important source of raw material because highly mesoporous ACs can be produced from waste tires rubber [24]. Mesopores AC is one of the most important characteristics in the liquid phase adsorption. Moreover, owing to the high surface areas (ranging from 164 to 1,260 m^2/g) and pore volumes (up to 1.62 cm^3/g), tire carbon are considered as a potential adsorbent for the removal of pollutants from wastewaters.

Rubber tire derived carbons were reported for the adsorption of aniline, p-Cl-aniline, p-toluidinem p-anisidine, cadmium ions and other toxic metals from wastewater using, onto waste-derived material with different textural and surface chemistry [25–27]. The removal of Cu(II) from wastewater by the batch adsorption technique using waste tire rubber ash as a low-cost adsorbent was also reported [28] with focus on the influence of pH, adsorbent dose, initial Cu(II) concentration and contact time on the removal of Cu (II) was studied. The kinetics of adsorption at different dose levels of adsorbent were also reported and the experimental data were analysed by the Langmuir and Freundlich isotherms and the corresponding sorption constants were evaluated. The scrap tires converted to granular ACs was reported to be capable of removing copper ions from industrial wastewater samples [29].

This work aims on the kinetic and computational analysis of the nickel uptake by AC prepared from rubber tires. The characterization of tire-based AC was carried out by determining the surface area, surface structure as well as adsorptive property.

2. Experimental work

2.1. Characterization

Scanning electron microscope (SEM) was used to characterize the morphology and microstructure of the produced AC. The SEM confirms the uniform structure of the produced materials. Energy-dispersive X-ray spectroscopy (EDX) was used to find out the type of elements presented in the produced AC. The EDX results confirmed the presence of carbon (89% weight) and oxygen (11% weight) elements in the tire-derived ACs. The surface area of AC was measured to be 465 m^2/g. This large surface area of the AC could play a factor in enhancing the removal of Ni(II).

2.2. Preparation of AC from rubber tires

Waste rubber tires were used to produce AC by the following procedure [6,7,15]. The waste rubber tire was collected, cleaned, washed with deionized water and then dried in an oven. The carbonization process follows this where the dried material was heated to approximately 500˚C for 6 h. This was followed by treatment with hydrogen peroxide solution for one day to oxidize adhering organic impurities. The material was washed with deionized water and dried in vacuum oven. The dried material was activated to 900˚C for 120 min. It was removed from the furnace and cooled in a desiccator. The material was then treated with 4-M nitric acid solution to remove the ash content and was then washed with deionized water. The product was finally dried in an oven and then characterized and tested for its sorption activity.

2.3. Adsorption procedure

The batch adsorption study was performed according to the following procedure. Fifty-millilitre Erlenmeyer flasks were used to carry out batch experiments in a thermostatic shaking water bath. Pollutants of known concentrations were taken in the flask to which suitable amount of adsorbent was added. The pH of the solution was altered using HCl or NaOH. Experiments were performed at fixed pH. Solutions were agitated mechanically in the water bath at desired temperature. The temperature was fixed between 25 and 35˚C for a fixed contact time period. Previous steps were repeated to optimize concentration of pollutant, particle size, pH, adsorbent dose, contact time and temperature by varying the values of different parameters. The solution was centrifuged, filtered and analysed by Atomic Absorption Spectroscopy (AAS) (in case of metal ions), UV–vis (in case of organic pollutants). The experiments were repeated three times and average values were reported. The pollutant uptake q_e (mol/g) was determined as follows in Eq. (1):

$$q_e = (C_0 - C)V/W \quad (1)$$

where C_0 and C are the initial and final concentrations of adsorbate (mol/L), respectively, V is the volume of solution (L) and W is the weight of adsorbent (g).

The kinetic study was conducted based on the following method. Fifty-millilitre Erlenmeyer flasks containing various amounts of standard solutions of pollutant was set-up and shaken in a thermostatic shaking water bath. A known amount of adsorbent was added to each flask. Flasks were agitated mechanically in the water bath at a constant temperature. Contact time, temperature and other conditions were selected based on preliminary experiments. The mixture was centrifuged at predetermined time intervals and the concentration of pollutant in the supernatant was analysed. Adsorbent particle size is an important variable in deciding centrifugation timings. The equilibrium concentration (C_e) and time to reach equilibrium were determined. Different adsorption models were investigated to find out the best representation of the kinetic data and adsorption parameters were determined.

Batch adsorption experiments were conducted by adding the 0.01 g of adsorbent to 100 mL of different Ni test solutions (15 ppm) in an Erlenmeyer flask (250 mL capacity). The flasks were agitated at different speed (0–150 rpm) in a rotary shaker for different duration of contact times (5–60 min). All experiments were conducted at 35, 45 and 55˚C. The initial and final concentrations of nickel were analysed using inductively coupled plasma mass spectrometry (ICP-MS). The experimental data based on 0.01 g of adsorbent added to 0.1 L of solution is presented in Tables 1 and 2.

The data were processed for applying the Langmuir and Freundlich isotherms equations. The equilibrium concentrations of adsorbate and the adsorption capacities are given in Table 3.

2.4. Computational study

Density functional theory (DFT) calculations using the quadratically convergent self-consistent field iterations [30] with the Los Alamos National Laboratory-2 double-ζ (LANL2DZ) basis set [31–33] were performed in order to elaborate on the kinetic adsorption of Ni^{2+} towards the possible active sites of the adsorbent. The

Table 1
Adsorption performance data of AC obtained from waste tires at different higher Ni concentrations

Amount of AC = 0.01 g				
	Ni initial conc (C_0)			
Time (m)	40 ppm	10 ppm	1 ppm	0.1 ppm
0	40	10	1	0.1
5	36.681	9.663	0.982	0.148
10	36.291	9.635	0.777	0.195
15	36.532	9.502	1.111	0.237
20	36.534	9.507	0.904	0.238
30	36.521	9.713	0.86	0.177
40	36.785	9.256	0.907	0.109
50	36.935	9.592	0.961	0.233
60	35.841	9.584	0.75	0.135

Table 2
Adsorption performance data of AC obtained from waste tires at different lower Ni concentrations

Amount of AC = 0.01 g				
	Ni initial conc (C_0)			
Time (m)	4 ppm	1 ppm	0.1 ppm	0.01 ppm
5	3.6681	0.9663	0.0982	0.0148
10	3.6291	0.9635	0.0777	0.0195
15	3.6532	0.9502	0.1111	0.0237
20	3.6534	0.9507	0.0904	0.0238
30	3.6521	0.9713	0.086	0.0177
40	3.6785	0.9256	0.0907	0.0109
50	3.6935	0.9592	0.0961	0.0233
60	3.5841	0.9584	0.075	0.0135

mono-binding nickel ion adsorptions on the functionalized pyrene system as a model (Fig. 4) were carried out using Gaussian 09 programme package [34]. The active sites considered in this work are the carbonyl oxygen of the carboxylic acid, the alcoholic oxygen of the carboxylic acid, the carbonyl oxygen and the oxygen of the alcohol group. The $Ni^{2+}\cdots\pi$-electron weak interaction was also considered as another common adsorption scenario. These sites/functional groups were selected based on the characterization results that confirmed their presence on the sorbents' surface. Full energy relaxations of the aforementioned computational model were performed and stationary points have been confirmed by frequency calculation. The initial binding energy was predicted according to Eq. (2) [35,36]:

$$BE_{Ni(II)\cdots Pyr} = E_{Pyr} + E_{Ni(II,tripletstate)} - E_{Ni(II)\cdots Pyr} \quad (2)$$

where BE is the mono-binding energy calculated in kcal/mol and E is the total energy in Hartrees.

3. Result and discussion

The equilibrium data presented in Fig. 1 were applied to Langmuir isotherm model and the equilibrium data presented in Fig. 2 were applied to Freundlich isotherm equation. The Langmuir isotherm is the most widely used two-parameter equation, commonly expressed as given in Eq. (3):

$$\frac{C_e}{q_e} = \frac{C_e}{Q_m} + \frac{1}{Q_m b} \quad (3)$$

where q_e is the amount adsorbed (mg/g), C_e the equilibrium concentration of the adsorbate (mg/L), Q_m the Langmuir constants related to maximum mono-layer adsorption capacity (mg/g) and b is the constant related to the free energy or net enthalpy of adsorption ($b \propto e^{-H/RT}$). The plots of C_e/q_e vs. C_e are shown in Fig. 1.

The data from this study showed that a straight line was obtained when C_e/q_e was plotted against C_e.

Table 3
Estimated adsorption capacities at different Ni concentrations

Initial conc. Ni (mg/L)			Conc. in soln. @ Equil.	Adsorption capacity					
C_0 (mg/L)	AC added (g)	Soln. vol. (L)	C_e (mg/L)	q_e (mg/g)	$1/C_e$	$1/q_e$	C_e/q_e	log C_e	log q_e
0.1	0.01	0.1	0.075	0.25	13.3333	4.0000	0.300	−1.125	−0.602
1	0.01	0.1	0.75	2.5	1.3333	0.4000	0.300	−0.125	0.398
4	0.01	0.1	3.584	4.16	0.2790	0.2404	0.862	0.554	0.619
10	0.01	0.1	9.256	7.44	0.1080	0.1344	1.244	0.966	0.872
40	0.01	0.1	36.76	32.4	0.0272	0.0309	1.135	1.565	1.511

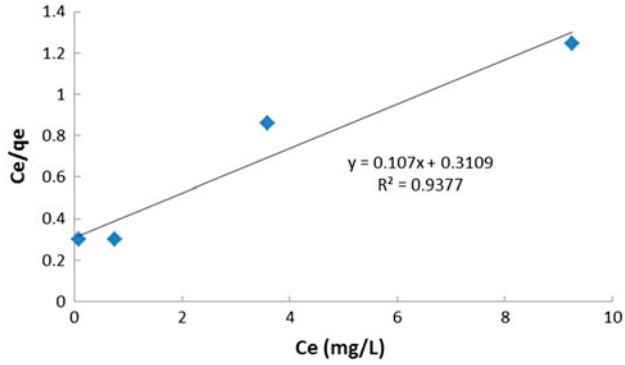

Fig. 1. Langmuir adsorption model fitting.

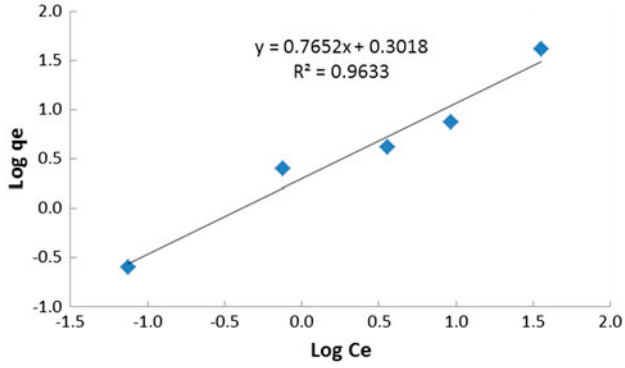

Fig. 2. Freundlich adsorption model fitting.

This indicates that the Langmuir isotherm was followed under the present conditions with $R^2 = 0.938$. The Langmuir parameters are tabulated in Table 4 and the overall absolute deviations between experimental and predicted values were found to be 14.4%.

The logarithmic form of Freundlich model is given by the following Eq. (4):

$$\log q_e = \log K_F + \log C_e \quad (4)$$

Therefore, plots of $\log q_e$ vs. $\log C_e$ (Fig. 2) were drawn to calculate the values of K_F and $1/n$ which are given in Table 3.

The experiments were performed in a standard way to generate data necessary for estimating kinetic parameters using standard kinetic models namely Langmuir and Freundlich. It was found that the data correlated very well with a correlation coefficient of 0.970 (Table 5). However, the overall absolute deviation between experimental and predicted values in Table 5 indicates that the data are not well correlated to Freundlich correlation coefficients compared to the

Table 4
Estimated values of Langmuir adsorption model parameters

Langmuir constants			
Slope	$1/Q_m$	0.107	
Constant	$1/Q_m b$	0.3109	
	Q_m	9.346	
	b	0.3442	
Adsorption capacity			
C_e (mg/L)	$q_{e,exp}$ (mg/g)	$q_{e,calc}$	% Dev
0.075	0.25	0.24	−5.93
0.75	2.5	1.92	−23.30
3.584	4.16	5.16	24.07
9.256	7.44	7.11	−4.40
Overall average absolute deviation (%)			14.43

Table 5
Estimated values of Langmuir adsorption model parameters

Slope	Intercept		
$1/n$	log K_F	n	K_F
Freundlich constants			
0.7652	0.3018	1.307	2.004
Adsorption capacity			
C_e (mg/L)	$q_{e,exp}$ (mg/g)	$q_{e,calc}$	% Dev
0.075	0.25	0.28	10.42
0.75	2.5	1.61	−35.69
3.584	4.16	5.32	27.91
9.256	7.44	11.00	47.82
Overall average absolute deviation (%)			30.46

Langmuir correlation coefficients. By comparing the results presented in Tables 4 and 5, it can be seen that the Langmuir model appears to fit accurately the adsorption of Ni onto the AC adsorbent. Moreover, these models are representing the isotherm data very well and the findings of our work are in agreement with the reported results in literature (19).

3.1. Characterization of the AC after adsorption

SEM and energy dispersive X-ray (EDX) analysis were performed to examine the surface morphology and the structure of the AC after adsorption, Fig. 3. In the EDX spectrum of the nickel-loaded AC, adsorption of nickel is indicated by the characteristic peaks for Ni (II) at 5.4 and 0.57 keV in addition to the peaks of the other elements constituting the AC.

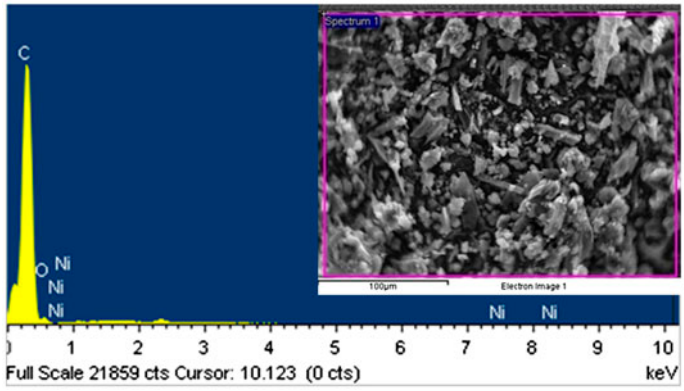

Fig. 3. The SEM image and EDX spectrum of the tire-derived carbonaceous adsorbent after adsorption of nickel and inset represent the SEM image of the same.

Table 6
Energy dispersive X-ray analysis (EDX) quantitative micro-analysis of the tire-derived AC after adsorption of nickel

Element	Weight %	Atomic %
C K	94.14	96.20
O K	4.70	3.50
Ni K	1.16	0.30
Totals	100.00	

The microanalysis spectrum of the components shown in Fig. 3 gives a clear sign of the presence of the nickel. The numerical results of EDX quantitative microanalysis, Table 6, indicate the presence of 1.16% nickel in the sample. It should be mentioned that such quantitative analysis is not highly reliable; however, it can be used as qualitative indication of the adsorption.

The FT-IR spectra of the carbon and of the carbon after the adsorption of Ni(II) is given in Fig. 4. The

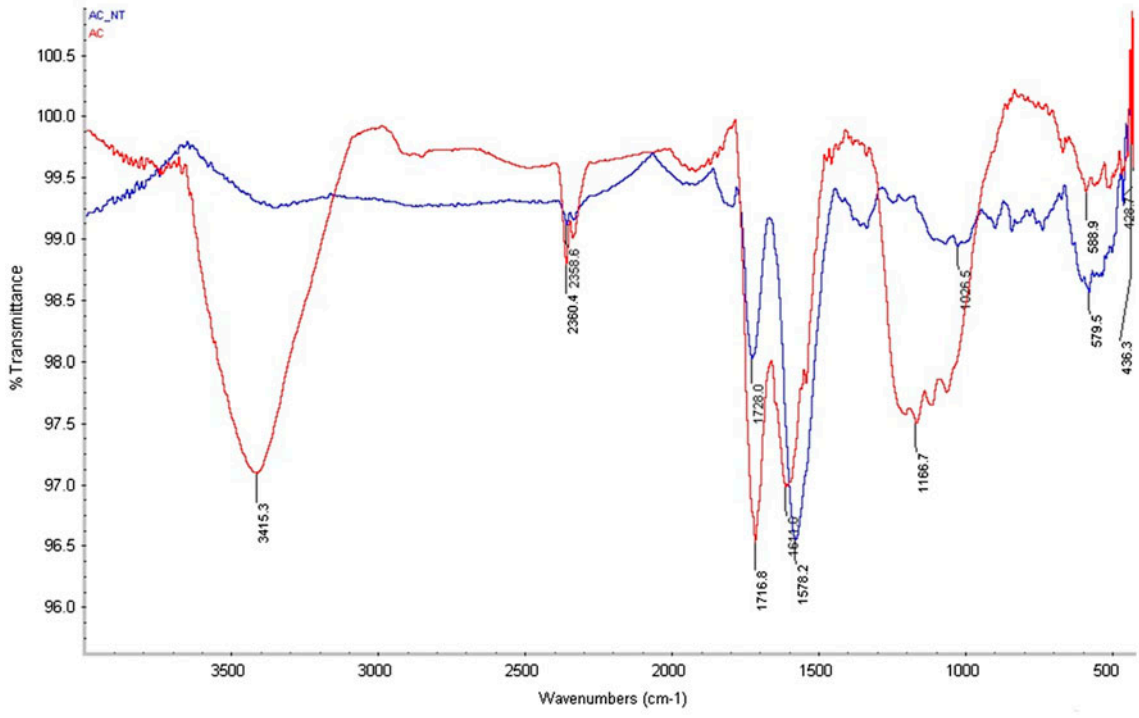

Fig. 4. FT-IR spectra of the carbon and of the carbon after the adsorption of Ni(II).

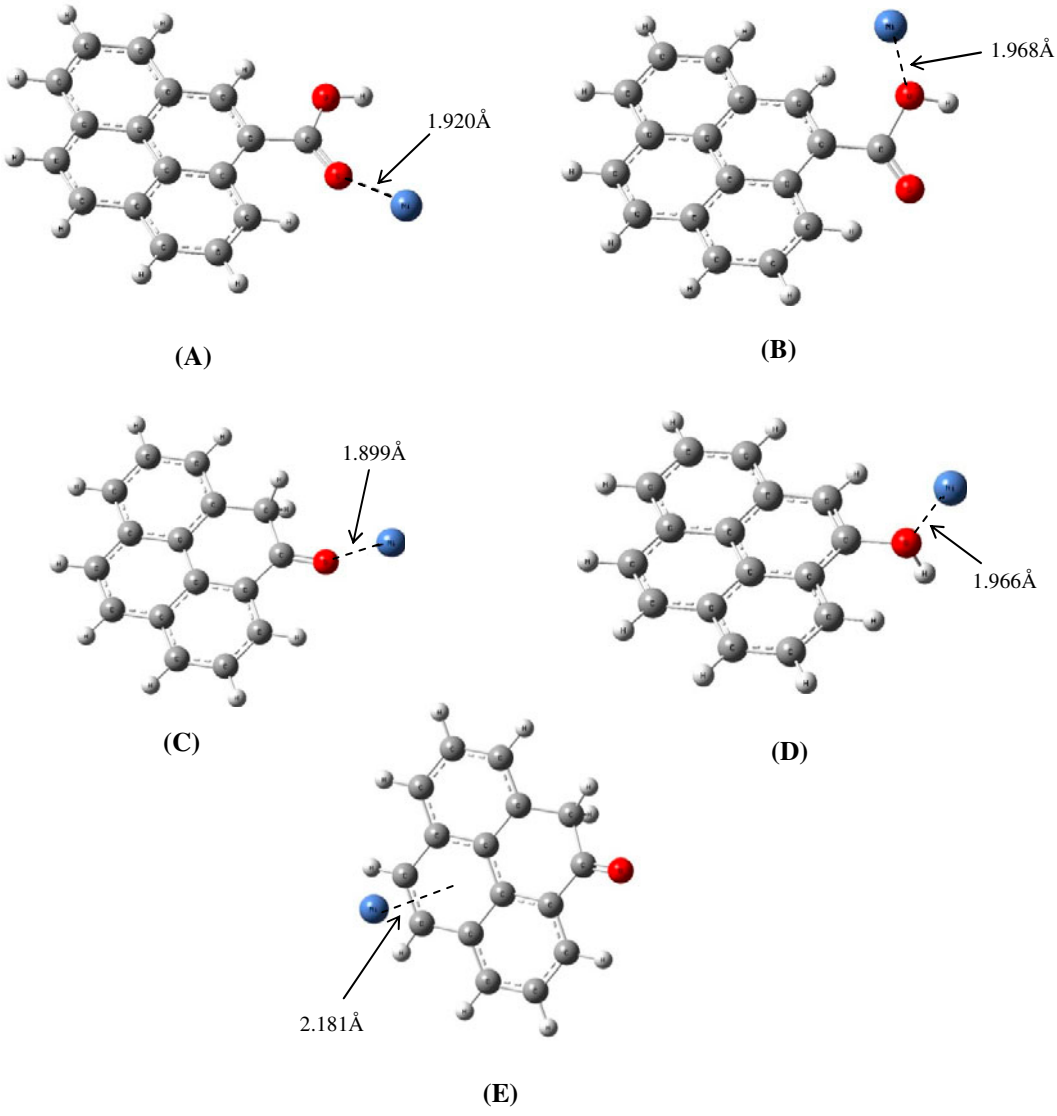

Fig. 5. Optimized mono-binding geometries of nickel ions with the carbonyl oxygen of the carboxylic acid (A), alcoholic oxygen of the carboxylic acid (B), carbonyl oxygen (C), alcoholic oxygen (D) and π-electron of the benzene rings (E) using the pyrene molecule as a model.

Table 7
Binding energies (kcal/mol) and bond distances (Å) of the mono-binding adsorption of the nickel ion on functionalized pyrenes as calculated at the B3LYP/LANL2DZ level of theory

Binding scenario[a]	Binding energy (kcal/mol)	Bond distance (Å)
Pyr-CO$^{(*)}$	258.2	1.899
Pyr-O$^{(*)}$H	257.2	1.966
Pyr-CO$^{(*)}$OH	262.9	1.920
Pyr-COO$^{(*)}$H	248.1	1.968
Pyr-$\pi^{(*)}$	221.1	2.181

[a]The binding site is represented with the asterisk$^{(*)}$.

spectrum clearly shows the adsorption of Ni(II) on the AC. The intense absorption peak around 1,716 cm^{-1} in AC represents the presence of carbonyl groups (C=O) which was significantly dimished after the adsorption of nickel metal as shown another FTIR spectrum. There was a broad and intense band around 1,000–1,200 cm^{-1} indicating the presence of C–O–C groups in AC that were almost lost after adsorption of nickel.

3.2. Computational data analysis

The optimized configurations representing the initial binding of Ni ions towards carboxylic acid (two possible positions on each oxygen atom), carbonyl, hydroxyl groups and diffuse π-systems of the benzene rings were computed in Fig. 5 and results listed in Table 7. The presence of oxygen surface groups such as carboxylic acid, carbonyl and hydroxyl on the surface of AC were confirmed by FTIR.

A mono-dentate binding energy of about of 250 kcal/mol was predicted, which is indicative of a possibly moderate chemisorption process. The nickel ion tends to approach much closer and more conveniently towards the carbonyl oxygen atom compared to the hydroxyl oxygen. This can be viewed by the slightly stronger calculated binding energy and shorter bond distance the nickel ion forms with the targeted oxygen atom Table 7. Although the interaction of the nickel ion towards the π-electrons on the benzene rings was predicted to be quite weaker, such type of interaction is still significant due to more probable positions in the AC materials for such an interaction.

4. Conclusion

This work was carried out to study the kinetic and computational analysis of the nickel uptake by the AC prepared from the waste rubber tire by physical activation method. The AC was characterized for the surface area, surface structure as well as adsorptive properties. A SEM showed differences in the surface morphology and the structure of the AC after adsorption. The EDX spectrum of the nickel-loaded AC showed the adsorption of nickel in the characteristic peaks for Ni(II) at 5.4 and 0.57 keV in addition to the peaks of the other elements constituting the AC. The kinetic studies were carried out to determine the kinetics of the adsorption process. The Langmuir isotherm was followed under the present conditions with $R^2 = 0.938$. The overall absolute deviations between experimental and predicted values were found to be 14.4%. The Langmuir model better appears to fit the adsorption of Ni onto AC adsorbent. The characterization and computational studies of the AC adsorbent after adsorption of nickel was also carried out and the results confirmed the positive adsorption process. FTIR analysis of AC before and after Ni adsorption indicated that adsorption of nickel metal on AC. The results showed the potential of AC in adsorbing nickel metal from aqueous solution.

Acknowledgements

The authors would like to acknowledge the support provided by King Abdulaziz City for Science and Technology (KACST) through the Science & Technology Unit at King Fahd University of Petroleum & Minerals (KFUPM) for funding this work through project No. 10-WAT1400-04 as part of the National Science, Technology and Innovation Plan (NSTIP).

References

[1] C.L. Mantell, Adsorption, McGraw-Hill Book Company, Inc., New York, NY, 1951.
[2] Y. Al-Degs, M.A.M. Khraisheh, S.J. Allen, M.N. Ahmad, Effect of carbon surface chemistry on the removal of reactive dyes from textile effluent, Water Res. 34 (2000) 927–935.
[3] R.C. Bansal, M. Goyal, Activated Carbon Adsorption, Taylor & Francis Group, Boca Raton, Fla., 2005.
[4] A.İ. Liapis, Fundamentals of Adsorption, Engineering Foundation, New York, NY, 1987.
[5] B.G. Linsen, Physical and Chemical Aspects of Adsorbents and Catalysts, Academic Press, London, 1970.
[6] D. Mohan, C.U. Pittman Jr., Activated carbons and low cost adsorbents for remediation of tri- and hexavalent chromium from water, J. Hazard. Mater. 137 (2006) 762–811.
[7] T.A. Saleh, V. Gupta, A.A. Al-Saadi, Adsorption of lead ions from aqueous solution using porous carbon derived from rubber tires: Experimental and computational study, J. Colloid Interface Sci. 396 (2013) 264–269.
[8] V.J.P. Poots, G. McKay, J.J. Healy, The removal of acid dye from effluent using natural adsorbents-II, Wood Water Res. 10 (1976) 1067–1070.
[9] A.K. Mittal, C. Venkobachar, Sorption and desorption of dyes by sulfonated coal, J. Environ. Eng. ASCE 119 (1993) 366–368.
[10] V.M.D. Chui, K.W. Mok, C.Y. Ng, B.P. Luong, K.K. Ma, Removal and recovery of copper(II), chromium(III), and nickel(II) from solutions using crude shrimp chitin packed in small columns, Environ. Int. 22 (1996) 463–468.
[11] G. McKay, M.S. Otterburn, J.A. Aga, Fuller's earth and fired clay as adsorbents for dyestuffs, Water Air Soil Pollut. 24 (1985) 307–322.
[12] C. Namasivayam, K. Periasamy, Bicarbonate-treated peanut hull carbon for mercury(II) removal from aqueous solution, Water Res. 27 (1993) 1663–1668.
[13] M.A. Ferro-García, J. Rivera-Utrilla, J. Rodríguez-Gordillo, I. Bautista- Toledo, Adsorption of zinc,

cadmium, and copper on activated carbons obtained from agricultural by-products, Carbon 26 (1988) 363–373.
[14] V.K Gupta, I. Ali, T.A. Saleh, M.N. Siddiqui, S. Agarwal, Chromium removal from water by activated carbon developed from waste rubber tires, Environ. Sci. Pollut. Res. 20 (2013) 1261–1268.
[15] T.A. Saleh, The influence of treatment temperature on the acidity of MWCNT oxidized by HNO_3 or a mixture of HNO_3/H_2SO_4, Appl. Surf. Sci. 257 (2011) 7746–7751.
[16] A. Olad, S. Ahmadi, A. Rashidzadeh, Removal of nickel(II) from aqueous solutions with polypyrrole modified clinoptilolite: Kinetic and isotherm studies, Desalin. Water Treat. 51(37–39) (2013) 7172–7180.
[17] A. Keränen, T. Leiviskä, A. Salakka, J. Tanskanen, Removal of nickel and vanadium from ammoniacal industrial wastewater by ion exchange and adsorption on activated carbon, Desalin. Water Treat. 53(10) (2015) 2645–2654.
[18] S. Haydar, M. Fayyaz Ahmad, G. Hussain, Evaluation of new biosorbents prepared from immobilized biomass of *Candida* sp. for the removal of nickel ions, 2015, doi:10.1080/19443994.2014.1003612.
[19] A. Ma, J.P. Barford, G. McKay, Application of the BDST model for nickel removal from effluents by ion exchange, Desalin. Water Treat. 52(40–42) (2014) 7866–7877.
[20] J.H. Tay, X.G. Chen, S. Jeyaseelan, N. Graham, Optimising the preparation of activated carbon from digested sewage sludge and coconut husk, Chemosphere 44 (2001) 45–51.
[21] M. Smisek, S. Cerny, Active Carbon, Elsevier, Amsterdam, 1970.
[22] C. Hsieh, H. Teng, Influence of mesopore volume and adsorbate size on adsorption capacities of activated carbons in aqueous solutions, Carbon 38 (2000) 863–869.
[23] K. Nakagawa, A. Namba, S.R. Mukai, H. Tamon, P. Ariyadejwanich, W. Tanthapanichakoon, Adsorption of phenol and reactive dye from aqueous solution on activated carbons derived from solid wastes, Water Res. 38 (2004) 1791–1798.
[24] P. Ariyadejwanich, W. Tanthapanichakoon, K. Nakagawa, S.R. Mukai, H. Tamon, Preparation and characterization of mesoporous activated carbon from waste tires, Carbon 41 (2003) 157–164.
[25] M. Xu, P. Hadi, G. Chen, G. McKay, Removal of cadmium ions from wastewater using innovative electronic waste-derived material, J. Hazard. Mater. 273 (2014) 118–123.
[26] M.G. Plaza, a.S. González, J.J. Pis, F. Rubiera, C. Pevida, Production of microporous biochars by single-step oxidation: Effect of activation conditions on CO_2 capture, Appl. Energy 114 (2014) 551–562.
[27] P. Hadi, J. Barford, G. McKay, Selective toxic metal uptake using an e-waste-based novel sorbent-single, binary and ternary systems, J. Environ. Chem. Eng. 2 (2014) 332–339.
[28] H.Z. Mousavi, A. Hosseynifar, V. Jahed, Removal of Cu(II) from wastewater by waste tire rubber ash, J. Serb. Chem. Soc. 75(6) (2010) 845–853.
[29] K.S. Ryoo, S. Kapila, Conversion of scrap tires to granular activated carbons and its evaluation as adsorbents, Environ. Eng. Res 2(2) (1997) 141–150.
[30] G.B.A. Bacskay, A quadratically convergent Hartree—Fock (QC-SCF) method. Application to closed shell systems, Chem. Phys. 61 (1981) 385–404.
[31] W.R. Wadt, P.J. Hay, Ab initio effective core potentials for molecular calculations. Potentials for the transition metal atoms Sc to Hg, J. Chem. Phys. 82 (1985) 270–283.
[32] W.R. Wadt, P.J. Hay, Ab initio effective core potentials for molecular calculations. Potentials for main group elements Na to Bi, J. Chem. Phys. 82 (1985) 284–298.
[33] W.R. Wadt, P.J. Hay, Ab initio effective core potentials for molecular calculations. Potentials for K to Au including the outermost core orbitals, J. Chem. Phys. 82 (1985) 299–310.
[34] M.J. Frisch, G.W. Trucks, H.B. Schlegel, G.E. Scuseria, M.A. Robb, J.R. Cheeseman, G. Scalmani, V. Barone, B. Mennucci, G.A. Petersson, H. Nakatsuji, M. Caricato, X. Li, H.P. Hratchian, A.F. Izmaylov, J. Bloino, G. Zheng, J.L. Sonnenberg, M. Hada, M. Ehara, K. Toyota, R. Fukuda, J. Hasegawa, M. Ishida, T. Nakajima, Y. Honda, O. Kitao, H. Nakai, T. Vreven, J.A. Montgomery Jr., J.E. Peralta, F. Ogliaro, M. Bearpark, J.J. Heyd, E. Brothers, K.N. Kudin, V.N. Staroverov, R. Kobayashi, J. Normand, K. Raghavachari, A. Rendell, J.C. Burant, S.S. Iyengar, J. Tomasi, M. Cossi, N. Rega, J.M. Millam, M. Klene, J.E. Knox, J.B. Cross, V. Bakken, C. Adamo, J. Jaramillo, R. Gomperts, R.E. Stratmann, O. Yazyev, A.J. Austin, R. Cammi, C. Pomelli, J.W. Ochterski, R.L. Martin, K. Morokuma, V.G. Zakrzewski, G.A. Voth, P. Salvador, J.J. Dannenberg, S. Dapprich, A.D. Daniels, Ö. Farkas, J.B. Foresman, J.V. Ortiz, J. Cioslowski, D.J. Fox, Gaussian 09, Revision D.01, Gaussian, Inc., Wallingford, CT, 2009.
[35] D.H. Chi, N.T. Cuong, N.A. Tuan, Y.T. Kim, H.T. Bao, T. Mitani, T. Ozaki, H. Nagao, Electronic structures of Pt clusters adsorbed on (5,5) single wall carbon nanotube, Chem. Phys. Lett. 432 (2006) 213–217.
[36] B. Padak, J. Wilcox, Understanding mercury binding on activated carbon, Carbon 47(12) (2009) 2855–2864.